

Chao XIE, Chaoqing DONG, Jicun REN

# Fluorescence cross-correlation spectroscopy using single wavelength laser

© Higher Education Press and Springer-Verlag 2009

**Abstract** In this paper, we first introduced the basic principle of fluorescence cross-correlation spectroscopy (FCCS) and then established an FCCS setup using a single wavelength laser. We systematically optimized the setup, and the detection volume reached about 0.7 fL. The home-built setup was successfully applied for the study of the binding reaction of human immunoglobulin G with goat antihuman immunoglobulin G. Using quantum dots (745 nm emission wavelength) and Rhodamine B (580 nm emission wavelength) as labeling probes and 532 nm laser beam as an excitation source, the cross-talk effect was almost completely suppressed. The molecule numbers in a highly focused volume, the concentration, and the diffusion time and hydrodynamic radii of the reaction products can be determined by FCCS system.

**Keywords** fluorescence cross-correlation spectroscopy, single-molecule detection, single laser excitation, quantum dot

With the rapid development of life sciences, people expect to study the conformational changes of biological macromolecules, the relationship between molecular structures and their functions at the single molecular level [1]. Furthermore, the molecular interaction is one of the research hotspots in this field [2, 3].

Currently, FCCS has become a powerful technique in single molecular detections due to its high sensitivity and short analysis times. This method has been used for measuring nucleic acid, protein conformational fluctuation [4–6], nucleic acid hybridization [7], protein interaction [8, 9], enzyme kinetics [10, 11], and the intracellular molecular interaction [12, 13]. Recently, some reviews have been published [14, 15], which introduced the theoretical background and improvements of FCCS.

Translated from *Chemical Journal of Chinese Universities*, 2008, 29(5) (in Chinese)

Chao XIE, Chaoqing DONG, Jicun REN (✉)  
College of Chemistry and Chemical Engineering, Shanghai Jiao Tong University, Shanghai 200240, China  
E-mail: jicunren@sjtu.edu.cn

To date, most FCCS systems use either dual-color lasers or two-photon excitation systems that make the FCCS structure to be complicated and costly since an expensive two-photon laser is needed. In this article, we established a setup of FCCS using single wavelength laser on the basis of a confocal configuration. Using quantum dots and fluorescence dyes as the probes, we studied the immune reaction of human immunoglobulin G with goat antihuman immunoglobulin G as a reaction model by FCCS system.

## 1 Theoretical background of FCCS

FCCS was developed on the basis of fluorescence autocorrelation spectroscopy. This method not only possesses high sensitivity, but it also overcomes the limit in which their diffusion coefficients must differ by a factor of at least 1.6, in order to distinguish the two components in fluorescence correlation spectroscopy (FCS) analysis. We already introduced the methodologies [20] and applications [21–24] of FCS. Here, we simply described the theoretical background of FCCS [7, 11]. In the model of FCCS, there are two separation light channels (denoted by 1, 2). The fluorescence intensity fluctuations in two channels can be analyzed by cross-correlation function:

$$G_{12}(\tau) = \frac{\langle \delta F_1(t) \delta F_2(t + \tau) \rangle}{\langle F_1(t) \rangle \langle F_2(t) \rangle} \quad (1)$$

Whereas the fluorescence fluctuation  $\delta F_1(t)$  is defined as the difference of the instantaneous fluorescence from the temporal mean in channel 1,  $\delta F_2(t + \tau)$  is defined as the difference of the instantaneous fluorescence from the temporal mean in channel 2 after lag  $\tau$  time. Taking into account the characteristics of the excitation and detection optics, a functional relation between the correlation function and the occupation times for translational diffusion for fluorescent species can be found.

$$G_{12}(\tau) = G_{12}(0) \left( 1 + \frac{\tau}{\tau_{D,12}} \right)^{-1} \left( 1 + \frac{\omega_0^2 \tau}{Z_0^2 \tau_{D,12}} \right)^{-\frac{1}{2}} \quad (2)$$

Whereas  $\tau_{D,12}$  is average lateral transit time of the two-color binding molecules, which is defined as the  $\tau$  value when  $G_{12}(\tau)$  is equal to  $G_{12}(0)/2$  as the same as in FCS model. The effective detection volume has an ellipsoidal shape. The  $\omega_0$  and  $Z_0$  are the horizontal and vertical axes (are defined as where laser power value descended to  $1/e^2$  from the center). Based on the above definition, the diffusion coefficient is then calculated on the basis of  $D = \omega_0^2 / (4\tau_{D,12})$ . According to the Stokes-Einstein relation  $R_h = kT / (6\pi\eta D)$ , we can get the hydrodynamic radius  $R_h$  of the two-color binding molecule, where,  $D$  is diffusion coefficient,  $k$  is Boltzmann constant ( $1.38 \times 10^{-23} \text{ J} \cdot \text{K}^{-1} \cdot \text{mol}^{-1}$ ),  $T$  is the absolute temperature, and  $\eta$  is the viscosity of the solvent.

In the experiment, fluorescence fluctuations of the two channels were simultaneously analyzed and cross-correlated. We first obtained the molecular number of channel 1 and 2 ( $N_{11}$  and  $N_{22}$ ) and then calculated the molecular number of two-color bounding complex ( $N_{12}$ ) based on following function:

$$N_{12} = 1 / [G_{12}(0) \cdot N_{11} \cdot N_{22}]$$

Finally, we obtained the concentration of two-color binding complex according to  $N_{12}$  and the detection volume (decided by  $\omega_0$  and  $Z_0$ ).

## 2 Experiments

### 2.1 Instrumentation and materials

The home-built FCCS system is shown in Fig. 1. In brief, the 532 nm YVO4 laser (Ion Laser Technology Co., Ltd. Shanghai) was attenuated by a circular neutral density filter (HB Optical Technology Co. Ltd. Shenyang). After it was expanded, the laser beam was reflected by a dichroic mirror (550DRLP, Omega Optical, USA) in an inverted fluorescence microscope (IX71, Olympus, Japan), after which, it was focused into a sample solution by a water immersion objective (UplanApo, 60×NA1.2, Olympus, Japan). About 30  $\mu\text{L}$  sample was placed on a cover slip (0.13–0.17 mm thickness, Sigma-Aldrich, USA). The excited fluorescence signal collected by the same objective passed through the dichroic mirror and then was split by another dichroic mirror (610DRLP, Omega Optical, USA). The short wavelength fluorescence was reflected by the mirror, filtered by a band-pass filter (565WB20, Omega Optical, USA), and finally collected after passing the 30  $\mu\text{m}$  pinhole by avalanche photodiodes (SPCM-AQR14, Perkin-Elmer EG&G, Canada). The long wavelength fluorescence passed through the mirror, filtered by a long-pass filter (700 ALP, Omega Optical, USA), and finally collected after passing the 70  $\mu\text{m}$  pinhole by another avalanche photodiodes. The yielded signals in the two channels were tracked and correlated by a real time correlator (ALV-5000/EPP, ALV-GmbH, Germany). The recording time per sample was 30 s. One mg/mL Rhodamine 6G and isothiocyanate Rhodamine B (Invitrogen Co.) solution were prepared and diluted according to the

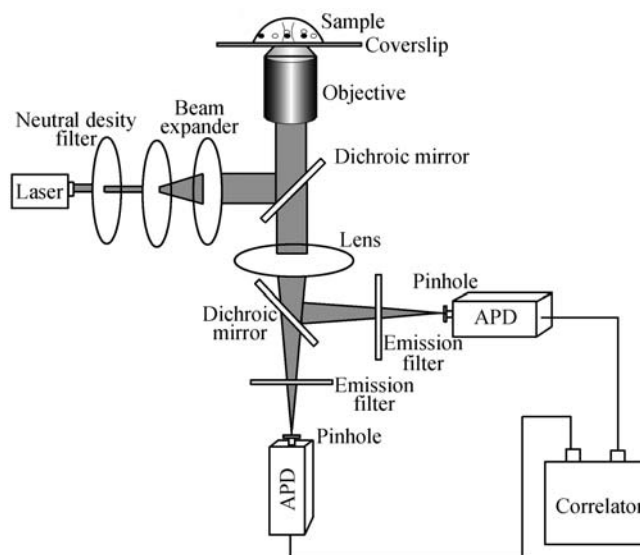


Fig. 1 FCCS setup with single wavelength laser

requirements of experiments. One mg/mL human immunoglobulin G and goat antihuman immunoglobulin G (Dingguo Biology Co. Ltd.) were prepared and kept at  $-20^\circ\text{C}$ . Water-soluble quantum dots (QD745, emission wavelength 745 nm) were prepared as described in the reference [25]. All solutions were prepared with ultrapure water (18.2 M $\Omega$ ) purified on Millipore Simplicity (Millipore).

### 2.2 Methods

IgG was labeled with isothiocyanate Rhodamine B (RBITC) in carbonate buffer (0.2 mmol/L, pH 9.16). IgG reacted with RBITC at room temperature for 3–5 h. The mixture was purified using ultrafiltration membrane (NMWL 50 000, Millipore) by centrifugation three times at 8000 rpm. In this process, the free dyes could be removed, which was characterized by capillary electrophoresis. The goat antihuman IgG was conjugated at room temperature with QD745 for 3–5 h based on the adsorption of QDs to antibody. The free QD745 could be removed using an ultrafiltration membrane (NMWL 100000, Millipore) by centrifugation three times at 8000 rpm. When the antibodies were mixed at the different ratios, the immunocomplexes was formed. Then, 30  $\mu\text{L}$  mixed solution was placed on a coverslip, and FCCS measurements were performed on a home-built FCCS system.

## 3 Results and discussion

### 3.1 FCCS system

In the FCCS assays, cross-talk effect, which is the fluorescence from one channel that can be detected in the other channel, significantly influences the reliability of

FCCS results. In order to avoid this effect, the dye-pair emission wavelengths must be markedly different. Unfortunately, these dye-pair are very rare. Therefore, two lasers are usually necessitated in the construction of FCCS system. However, in two lasers FCCS system, we meet the problem on how to adjust two laser focuses to overlap.

In this article, the 532 nm laser beam was used as the excitation source. Quantum dots (745 nm) and Rhodamine B (580 nm) were used as fluorescence probes. Single wavelength laser FCCS was successfully realized due to the use of unique optical property of quantum dots. Quantum dots can be excited at a wide wavelength range since they have broad absorption spectra. In this study, QD745 can be excited by 532 nm laser, and the maximum emission wavelength is at 745 nm. The photoluminescence spectra of Rhodamine B and QD745 as well as the transmission spectral curves of the filter and mirror are shown in Fig. 2. The 610-nm dichroic mirror was used to split the fluorescence. The light in channels 1 and 2 were filtered by a 565 WB 20 band-pass filter and 700 nm long-pass filter. In this case, the cross-talk effect was near-completely suppressed. The results indicated that the fluorescence intensity ratio of Rhodamine B in channel 2 to channel 1 was 1/12 and the fluorescence intensity ratio of QD745 in the channel 1 to the channel 2 was 1/80.

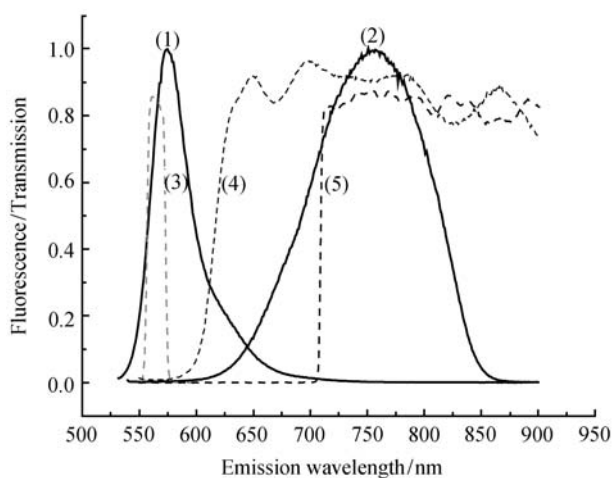


**Fig. 2** Emission spectra of Rhodamine B and QD745

(1) Emission spectra of Rhodamine B, (2) Emission spectra of QD745, (3) Emission filter for channel 1, (4) Dichroic mirror, (5) Emission filter for channel 2

Figure 3 shows the correlation curves of immune complex including three curves. Curve 1 is the fluorescence autocorrelation curve of Rhodamine B, curve 2 is the fluorescence autocorrelation curve of QD745 and curve 3 is the FCCS curve of immune complex.

### 3.2 Detection Volume

The accurate measurement of the detection volume is the precondition to calculate the molecule concentration. The

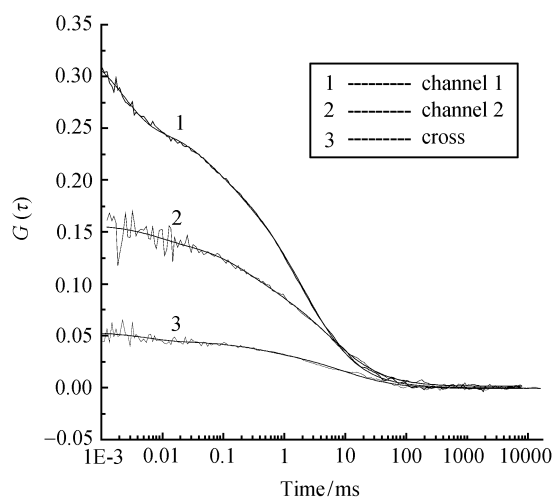


**Fig. 3** FCS curves in channel 1, 2 and FCCS curve

structure parameter  $z_0/\omega_0$  were determined using  $1.0 \times 10^{-8}$  mol/L Rhodamine 6G, assuming its diffusion constant of  $D = 2.8 \times 10^{-6}$  cm<sup>2</sup>/s in water. The recording time was 30 s repeated 11 times. The data were plugged into formula 2. The obtained  $\omega_0$  and  $z_0$  were 0.26  $\mu$ m and 1.89  $\mu$ m, and their RSDs were 0.8 % and 5.6 % ( $n = 11$ ) respectively. The detection volume in channel 1 was 0.7 fL according to the formula  $V_{eff} = \pi^{3/2} \omega_0^2 z_0$  [7].

Since it is very difficult to find a conventional organic dye whose excitation wavelength is 532 nm and emission wavelength is more than 700 nm, the above method cannot be used to measure the detection volume in channel 2. Instead, we used an indirect method to measure the detection volume in channel 2. In detail, Rhodamine B was first used to determine the detection volume on a 590-nm long-pass filter in the same method as the method described above. After which, the Rhodamine B sample was replaced by QD745; the number of particles was recorded in the same condition. Last, 590 nm long-pass filter was replaced by 700 nm long-pass filter; the number of QD745 particles was recorded again. Based on the ratio of the particle numbers in twice measurements, the volume in channel 2 could be obtained indirectly to be 1.5 fL.

Since it was dependent on the intersection of two channels, the detection volume in FCCS system about was 0.7 fL, which was decided by the smaller volume in two channels.

### 3.3 Reproducibility

The labeled human immunoglobulin G was mixed with goat antihuman immunoglobulin G at the different ratios, and the mixture was determined after dilution with a buffer. To study the reproducibility of our system, the samples were determined seven times. The concentrations of the complex were calculated on the basis of the formula

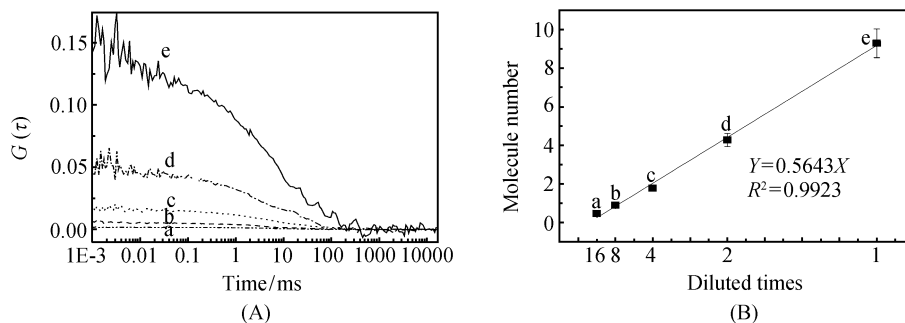


**Fig. 4** FCCS curves of reaction products (A) and relationship between molecular number and diluting times of the solution after the binding reaction (B). Concentration of reaction product/ ( $\text{mol}\cdot\text{L}^{-1}$ ): (a)  $1.14\times 10^{-9}$ ; (b)  $2.07\times 10^{-9}$ ; (c)  $4.27\times 10^{-9}$ ; (d)  $1.02\times 10^{-8}$ ; (e)  $2.21\times 10^{-8}$

$C_{12} = \frac{N_{12}}{V * N_A}$ , where  $V$  is cross volume, and  $N_A$  is Avogadro's constant. The results showed that this method has good reproducibility, and the RSD of the concentrations was less than 8.2%.

### 3.4 Reliability

The immune complexes were analyzed by FCCS after they were diluted to various concentrations. The results are shown in Fig. 4(A). The amplitude  $G_{12}(0)$  increased with the increase of immune complex concentration. A good linear relation ( $R^2=0.992$ ) was obtained by plotting the molecular number to dilution times [Fig. 4(B)]. The molecular number in the detection volume is 0.4–10. This data illustrated that our FCCS system was an effective one.

The Normalized FCCS curves are shown in Fig. 5, which were obtained by normalized treatment from Fig. 4. We observed that different concentration complex had the same diffusion coefficient ( $\tau_{D,12}$  ( $4.138\pm 0.019$ ) ms). This result illustrated that the conformation of the complex had no change. The diffusion coefficient was calculated to be  $4.08\times 10^{-12}$   $\text{m}^2/\text{s}$ , and the hydrodynamic radius of the reaction product was about 54 nm.

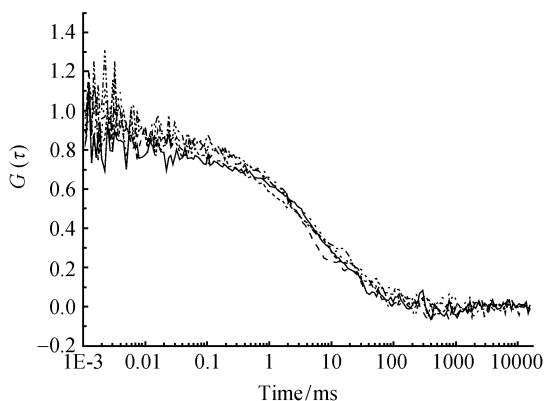


**Fig. 5** Normalized FCCS curves of the immune complex

## 4 Conclusion

In this article, we established a setup of single wavelength FCCS and systematically investigated some parameters of the FCCS system. Using this system we successfully obtained the molecule number concentration, diffusion coefficient, and hydrodynamic radius of the immune complex. Our results demonstrated that single wavelength FCCS was easily realized and the cross-talk effect was almost completely suppressed by using quantum dots as labeling probes.

## References

- Shao C, Hu D H, Sun H Z, Yan L K, Su Z M, Wang R S, Zhu W S, Guo J H, Sun N Z, Sun H, Li Z S, Sun C C. Structure exploration and function prediction of SARS coronavirus E protein. *Chem Res Chinese U*, 2005, 26(8): 1512–1516 (in Chinese)
- Zhao J W, Wang N. Electricity characterization of metalloprotein at molecular level by conducting atomic force microscopy. *Chem Res Chinese U*, 2005, 26(4): 745–753 (in Chinese)
- Nie S, Chen P, Liang S P. Identification of interacting molecules by biomolecular interaction analysis combined with surface plasmon resonance-mass spectrometry at 10–15 mol Level. *Chem Res Chinese U*, 2005, 26(1): 68–72 (in Chinese)
- Heikai A A, Heikal S T, Baird G S, Tsien R Y, Webb W W. Molecular spectroscopy and dynamics of intrinsically fluorescent proteins: Coral Red (dsRed) and Yellow (Citrine). *Proc Natl Acad Sci*, 2000, 97(22): 11996–12001
- Torres T, Levitus M. Measuring conformational dynamics: A new FCS-FRET approach. *J Phys Chem B*, 2007, 111(25): 7392–7400
- Wennmalm S, Edman L, Rigler R. Conformational fluctuations in single DNA molecules. *Proc Natl Acad Sci*, 1997, 94(20): 10641–10646
- Schwille P, Meyer-Almes F J, Rigler R. Dual-color fluorescence cross-correlation spectroscopy for multicomponent diffusional analysis in solution. *J Biophys*, 1997, 72(4): 1878–1886
- Larson D R, Gosse J A, Holowka D A, Baird B A, Webb W W. Temporally resolved interactions between antigen-stimulated IgE receptors and lyn kinase on living cells. *J Cell Biol*, 2005, 171(3):

527–536

9. Oyama R, Takashima H, Yonezawa M, Doi N, Miyamoto-Sato E, Kinjo M, Yanagawa H. Protein-protein interaction analysis by c-terminally specific fluorescence labeling and fluorescence cross-correlation spectroscopy. *Nucleic Acids Res*, 2006, 34(14): e102
10. Kettling U, Koltermann A, Schwille P, Eigen M. Real-time enzyme kinetics monitored by dual-color fluorescence cross-correlation spectroscopy. *Proc Natl Acad Sci*, 1998, 95(4): 1416–1420
11. Rarbach M, Kettling U, Koltermann A, Eigen M. Dual-color fluorescence cross-correlation spectroscopy for monitoring the kinetics of enzyme-catalyzed reactions. *Methods*, 2001, 24(2): 104–116
12. Bacia K, Schwille P. Dynamic view of cellular processes by in vivo fluorescence auto- and cross-correlation spectroscopy. *Methods*, 2003, 29 (1): 74–85
13. Bacia K, Kim S A, Schwille P. Fluorescence cross-correlation spectroscopy in living cells. *Nat Methods*, 2006, 3(2): 83–89
14. Kim S A, Heinze K G, Waxham M N, Schwille P. Intracellular calmodulin availability accessed with two-photon cross-correlation. *Proc Natl Acad Sci*, 2004, 101(1): 105–110
15. Wohland T, Hwang L C. Recent advances in fluorescence cross-correlation spectroscopy. *Cell Biochem Biophys*, 2007, 49(1): 1–13
16. Magde D, Elson E L, Webb W W. Thermodynamic fluctuations in a reacting system: measurements by fluorescence correlation spectroscopy. *Phys Rev Lett*, 1972, 29(11): 705–708
17. Rigler R, Mets U. Diffusion of single molecules through a gaussian laser beam. *Soc Photo-Opt Instrum Eng*, 1992, 1921 (1): 239–248
18. Rigler R, Mets U, Widengren J, Kask P. Fluorescence correlation spectroscopy with high count rates and low background: analysis of translational diffusion. *Eur Biophys J*, 1993, 22(3): 169–175
19. Eigen M, Rigler R. Sorting Single Molecules: Application to diagnostics and evolutionary biotechnology. *Proc Natl Acad Sci*, 1994, 91(13): 5740–5747
20. Zhang P D, Ren J C. Advances in fluorescence correlation spectroscopy and its applications in single molecule detection. *Chinese J Anal Chem*, 2005, 33(6): 875–880 (in Chinese)
21. Dong C Q, Bi R, Qian H F, Li L, Ren J C. Coupling fluorescence correlation spectroscopy with microchip electrophoresis to determine the effective surface charge of water-soluble quantum dots. *Small*, 2006, 2(4): 534–538
22. Dong C Q, Qian H F, Fang N F, Ren J C. Study of fluorescence quenching and dialysis process of cdte quantum dots, using ensemble techniques and fluorescence correlation spectroscopy. *J Phys Chem B*, 2006, 110(23): 11069–11075
23. Dong C Q, Zhang P D, Bi R, Ren J C. Characterization of solution-phase DNA hybridization by fluorescence autocorrelation spectroscopy: genotyping of C677T from methylene tetrahydrofolate reductase gene. *Talanta*, 2007, 70(71): 1192–1197
24. Dong C Q, Ren J C. On-line investigation of laser-induced aggregation and photo-activation of cdte quantum dots by fluorescence correlation spectroscopy. *J Phys Chem C*, 2007, 111 (22): 7918–7923
25. Qian H F, Dong C Q, Peng J L, Qiu X, Xu Y H, Ren J C. High-quality and water-soluble near-infrared photoluminescent CdHgTe/CdS quantum dots prepared by adjusting size and composition. *J Phys Chem C*, 2007, 111 (45): 16852–16857